

# BLADING DESIGN FOR NARROW RADIAL FLOW IMPELLER OR GUIDE WHEEL BY USING SINGULARITY CARRIER AUXILIARY CURVES

By

O. FŰZY

Department of Hydraulic Machinery, Polytechnical University, Budapest

(Received May 11, 1966)

Presented by Prof. Dr. J. VARGA

As it is well known, any blade or cascade design can make use of an appropriately selected singularity carrier curve which is not entirely within the blade profile [1]. Such a curve — the so-called singularity carrier auxiliary curve — cannot be considered as physically feasible since the usual, physically feasible singularity carrier curve sections are entirely within the profile [2], [3], [4]. Employment of the singularity carrier auxiliary curve, similarly to that of the physically feasible one, is absolutely correct, thus it differs theoretically from the methods [5, 6] where the physically feasible curve is approximated by a simpler curve in order to simplify calculations.

Adaptation of the singularity carrier auxiliary curve for the design and dimensioning of a straight plane cascade is found in reference [7]. The contents of this paper will be considered here as known and, therefore, used for the design of narrow radial flow impeller or guide wheel bladings.

Since narrow radial flow impellers are being dealt with, considerations are restricted to the determination of the sections of blades on an axisymmetric stream surface.

The ideas concerning impellers may be applied to steady guide wheels by substituting  $\omega = 0$ . The thickness of the thin blades may be prescribed and there is a relatively simple possibility existing for the determination of the distribution of sources required for their production.

The existence theorems discussed in detail by reference [1] make a more general study of the problem possible. However, the general solution will be discussed in a subsequent paper.

## Symbols

$r, \varphi$	= cylindrical coordinates in the impeller
$z$	= impeller blade number
$c$	= absolute velocity in the impeller
$Q$	= flow through the impeller
$H$	= impeller delivery head
$\eta_h$	= hydraulic efficiency of the impeller

- $b$  = impeller width  
 $\omega$  = angular velocity of the impeller  
 $\xi, \eta$  = co-ordinates in plane  $\zeta$   
 $t$  = straight cascade pitch  
 $c_\zeta$  = absolute velocity in plane  $\zeta$   
 $c_\xi, c_\eta$  = components of  $c_\zeta$   
 $u_\eta$  = the image of peripheral velocity  $u$  in plane  $\zeta$   
 $\Gamma$  = blade circulation  
 $\Gamma_p$  = the circulation of prerotation  
 $c_{k\eta} = \Gamma/2t$   
 $c_{p\eta} = \Gamma_p/zt$   
 $\gamma_x, q_x$  = distributions along the chord  
 $\gamma_\xi^*, q_\xi^*$  = dimensionless function used for the production of  $\gamma_x$  and  $q_x$   
 $\gamma_s, q_s$  = distributions along curve  $S$   
 $w_x, w_y$  = components of the image in plane  $\zeta$  of the relative velocity in direction  $x$  and  $y$   
 $x, y$  = coordinates parallel and normal to chord  
 $c_L$  = velocity induced by blades  
 $\tau$  = thickness of blades  
 $\gamma_s$  = coordinate of curve  $S$

$$n_{qe} = n Q^{1/2} \left( \frac{H}{\eta_h} \right)^{-3/4}$$

$$v_e = \frac{2gH}{\eta_h u_2^2}$$

### Fundamental relations

The blade profiles will be determined on a surface of revolution characterized by a middle position (A—A in Fig. 1).

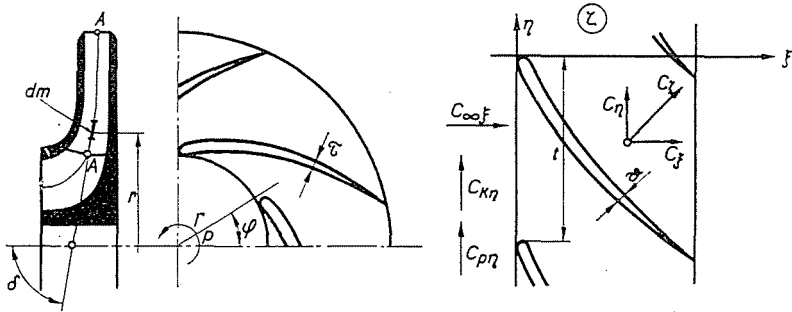


Fig. 1

The surface of revolution will be mapped out in the usual manner [4, 5] by means of the functions providing a conformal representation

$$\eta = \frac{zt}{2\pi} \varphi \quad (1/a)$$

and

$$\xi = \frac{zt}{2\pi} \int_{r_1}^r \frac{dm}{r} \quad (1/b)$$

Here  $z$  represents the number of blades, and  $t$  a length optionally selected. After mapping out the family of blade sections will appear within the  $\xi, \eta$  coordinate system, in plane  $\zeta$ , as an infinite straight plane cascade of  $t$  pitch. Between the absolute velocity  $c$  in the impeller and velocity in the straight cascade  $c_\zeta$  the well-known

$$c = \frac{zt}{2r\pi} c_\zeta \quad (2)$$

relation will exist [4].

The flow in plane  $\zeta$  is produced in the well-known manner, that is, as the sum of a basic flow and the induced flow generated by the blades but using, for the determination of the latter, a singularity carrier auxiliary curve [7]. Since the width of the impeller  $b(r)$  is not required to remain constant,

$$\nabla c_\zeta = -c_\zeta \frac{\partial}{\partial \xi} \ln b \quad (3)$$

which means that there is a continuous distribution of sources [4].

Satisfying Equations (3) with the integral averages taken only in the direction of coordinate  $\eta$ , the  $\xi$ -direction component of the basic flow with sources would be represented [3, 8] by

$$c_{g\xi} = \frac{Q}{bzt} + \frac{\Gamma}{t} \left[ \frac{1}{b} \int_0^{\xi^*} b q_\xi^* d\xi^* - \int_0^{\xi^*} q_\xi^* d\xi^* + \frac{1}{2} \int_0^1 q_\xi^* d\xi^* \right] \approx \frac{Q}{bzt} \quad (4)$$

If the circulation of the vortex preceding the impeller is  $\Gamma_p$ , then the  $\eta$ -direction component of the basic flow will be

$$c_{g\eta} = c_{p\eta} + c_{k\eta} \quad (5)$$

where

$$c_{p\eta} = \Gamma_p/zt, \quad c_{k\eta} = \Gamma/2t, \quad \text{and } \Gamma = 2\pi gH/\eta_h z \omega.$$

In order to produce the flow induced by blades, the chord of the physically feasible  $S$  singularity carrier curve, as a singularity carrier auxiliary curve, will be made use of: distributions  $\gamma_s(s)$  and  $q_s(s)$  pertaining to curve  $S$  will be substituted by distributions  $\gamma_x(x)$  and  $q_x(x)$  located on the chord. On the other hand, by using the symbols of Fig. 2, distributions  $\gamma_x(x)$  and  $q_x(x)$  are traced back through expressions

$$\gamma_x(\xi^*) = \frac{\Gamma}{\xi_2 \sqrt{1 + \tan^2 \beta_0}} \gamma_\xi^*(\xi^*) \quad (6/a)$$

and

$$q_x(\xi^*) = \frac{\Gamma}{\xi_2 \sqrt{1 + \tan^2 \beta_0}} q_\xi^*(\xi^*) \quad (6/b)$$

to the dimensionless functions  $\gamma_\xi^*(\xi^*)$  and  $q_\xi^*(\xi^*)$ .

The velocity normal to curve  $S$  is everywhere  $q_s/2$ , whereas that normal to the chord will be indicated by

$$w_y = v_y \pm \frac{q_x}{2} \quad (7/a)$$

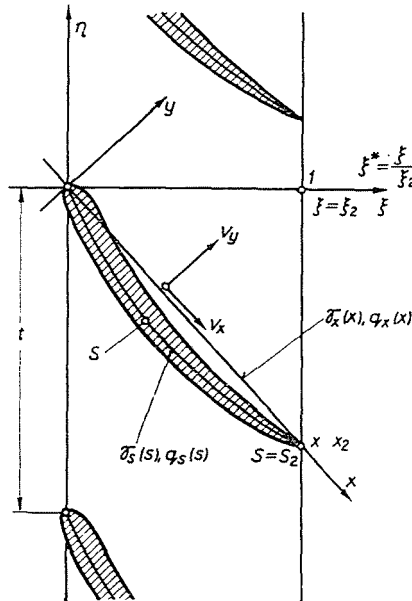


Fig. 2

and that parallel to the chord by

$$w_x = v_x \mp \frac{q_x}{2} \quad (7/b)$$

with the remark, however, that the top sign applies to the side of the chord marked "f", and the bottom one to that marked "a".

Considering the straight cascade pattern of the steady absolute flow within the impeller as having velocity potential, the relative flow pattern (Fig. 1) is:

$$\frac{\partial w_y}{\partial x} - \frac{\partial w_x}{\partial y} = 2w \sin \delta \left[ \frac{2r\pi}{zt} \right]^2 = \Omega \quad (8/a)$$

or, with respect to the source character of the flow,

$$\frac{\partial w_x}{\partial x} + \frac{\partial w_y}{\partial y} = -c_\xi \frac{\partial}{\partial \xi} \ln b = D. \quad (8/b)$$

As is well known, the condition of an enclosed profile is

$$\int_0^{S_2} b q_s ds = 0 \quad (9)$$

which is associated, in a straight cascade, with the condition:

$$\int_0^{x_2} b q_x dx = 0. \quad (10)$$

### Determination of the singularity carrier chord

In connection with the singularity carrier chord, the existence theorems well known from references in the literature [1, 7] must be satisfied. Functions  $\gamma_x(x)$  and  $q_x(x)$  must be analytical over the open interval  $I(0 < x < x_2)$  — which applies a specification to functions  $\gamma_\xi^*(\xi^*)$  and  $q_\xi^*(\xi^*)$  as well, and curve S must be within the circle drawn over the chord as a diameter. The satisfaction of these conditions does not cause any difficulties.

The terminals of curve S and its chord coincide which means that, by taking Equation (10) into consideration,

$$\int_0^{x_2} b v_y dx = 0. \quad (11)$$

With the influence functions known from references [4] introduced, the  $\xi$  and  $\eta$  components [7] of the velocity induced by the blades — apart from local velocity difference on the chord — is given by integrals

$$\begin{aligned} c_{L\xi}(\xi^*) &= \frac{\Gamma}{t} \int_0^1 \left[ \gamma_\xi^*(\xi^{*'}) \Phi \left( \frac{\xi - \xi'}{t}, \frac{\eta - \eta'}{t} \right) + \right. \\ &\quad \left. + q_\xi^*(\xi^{*'}) \Psi \left( \frac{\xi - \xi'}{t}, \frac{\eta - \eta'}{t} \right) \right] d\xi^{*'}, \end{aligned} \quad (12/a)$$

and

$$\begin{aligned} c_{L\eta}(\xi^*) &= \frac{\Gamma}{t} \int_0^1 \left[ \gamma_\xi^*(\xi^{*'}) \Psi \left( \frac{\xi - \xi'}{t}, \frac{\eta - \eta'}{t} \right) - \right. \\ &\quad \left. - q_\xi^*(\xi^{*'}) \Phi \left( \frac{\xi - \xi'}{t}, \frac{\eta - \eta'}{t} \right) \right] d\xi^{*'}, \end{aligned} \quad (12/b)$$

where the Cauchy's principal value should be calculated.

Furthermore, with the  $u_\eta = u \ 2 \ r \ \pi/zt$  image of the peripheral velocity  $u$  is also introduced [4],

$$v_y = \frac{1}{\sqrt{1 + \tan^2 \beta_0}} [c_{p\eta} + c_{k\eta} - u_\eta + c_{L\eta} - \tan \beta_0 c_{L\xi} - \tan \beta_0 c_{g\xi}] \quad (13/a)$$

and

$$v_x = \frac{1}{\sqrt{1 + \tan^2 \beta_0}} [c_{g\xi} + c_{L\xi} + \tan \beta_0 (c_{p\eta} + c_{k\eta} - u_\eta + c_{L\eta})] \quad (13/b)$$

Now allow the principal dimensions optionally selected, within certain limitations, in course of blading design to change. Starting from this idea, let us introduce equation

$$b(r) = \varkappa b_0(r) \quad (14)$$

for the  $b(r)$  width distribution, where  $b_0(r)$  represents the distribution when the principal dimensions were previously calculated. The factor  $\varkappa$  in Equation (14) may be determined by condition (11), on the basis of Equation (13), by the following formula:

$$\varkappa = \frac{Q \tan \beta_0}{zt \int_0^1 b_0 (c_{p\eta} + c_{k\eta} - u_\eta + c_{L\eta} - \tan \beta_0 c_{L\xi}) d\xi^*} \quad (15)$$

Thus with a line of  $\beta_0$  angle taken and velocity components  $c_{L\xi}$  and  $c_{L\eta}$  determined by making use of Equations (12) then calculating factor  $\varkappa$  from Equation (15), the straight section will actually represent the chord of curve  $S$ , if distribution  $b(r)$  as given by (14) is employed. The possible  $\beta_0$  values include a version where  $\varkappa = 1$  and, therefore, no principal dimension modification is required. According to experiences of numerical calculations, this value is well approximated by the chord angle pertaining to the blading of infinite number of blades which means that in the case of its application  $\varkappa$  will approximate unit and, consequently, principal dimension modification according to (14) would cause no difficulties, whatsoever. Accordingly,

$$\tan \beta_0 = \frac{\eta_{2\infty}}{\xi_2} \quad (16)$$

where [4]

$$\eta_{2\infty} = \frac{zt \xi_2}{Q} \int_0^1 b_0 \left[ c_{p\eta} - u_\eta + \frac{r}{t} \int_0^{\xi^{**}} \gamma_{\xi'}^* (\xi^{**}) d\xi^{**} \right] d\xi^* \quad (17)$$

Calculating  $\tan \beta_0$  by means of Equations (17) and (16) the value of  $\alpha$  will be given by (15). Making use of this method, distribution  $b(r)$  can be calculated by means of Equation (14) and, thereby, the chord of the unknown curve  $S$ , that is, the singularity carrier auxiliary curve is obtained.

### Determination of the physically feasible singularity carrier curve

For the determination of curve  $S$ , the idea described in connection with slightly cambered cascades will be followed [7]. Accordingly, the continuity equation will be determined for curve II (Fig. 3) with the analytical continuation of the flow pattern through the chord up to curve  $S$ , then for curve I by extending the analytical continuation through curve  $S$  to the chord.

Using the symbols of Fig. 3 the following expression applies to curve II

$$\int_0^x b(x) \left( -v_y - \frac{q_x}{2} \right) dx + \int_0^S b(s) \frac{q_s}{2} ds \cong -b(x, 0) \int_0^{y_s} w_{x,f}(x, y) dy \quad (18)$$

at the right hand side of which, with respect to the slight camber, the approximation  $b(x, y) \cong b(x, 0)$  was made use of.

Similarly, the following relation can be written for curve I:

$$\int_0^x b(x) \left( -v_y + \frac{q_x}{2} \right) dx - \int_0^S b(s) \frac{q_s}{2} ds \cong -b(x, 0) \int_0^{y_s} w_{x,a}(x, y) dy. \quad (19)$$

By producing the velocities in Taylor's expansion at the right hand side of Equations (18) and (19), integration can be followed out until  $|y_s|$  will be smaller than the shorter one of the pertaining lengths  $|x|$  and  $|x - x_2|$  respectively, that is, until curve  $S$  is within the square drawn over the chord as its diagonal. This condition must be specified in order to ensure the convergence of the Taylor's series since the velocity distribution function exhibits singularity at the points  $x = 0$  and  $x = x_2$ , respectively. According to the experiences in gathered numerical calculations, this condition is satisfied in practice. Expansion is performed at the right hand side of Equations (18) and (19) then, following integration, the  $y$  derivatives are expressed by derivatives according to  $x$  using Equations (8) and, finally, Equations (7) are substituted. By adding up and then subtracting the two equations thus obtained





these series after the members indicated. Satisfactory approximation may be achieved in many cases even with only the first two members of Equation (20) and only the first member of the right hand side of Equation (23) being taken into consideration. In this case distribution  $q_x$  pertaining to the given  $F(x)$  can be determined by making use of Equation (23), and the points of curve  $S$  are given by the product of those minimum absolute value roots of Equations (20) for which, in case of any  $0 < x < x_2$ , the chord is:

$$\lim_{\varepsilon \rightarrow 0} [y_s(x + \varepsilon) - y_s(x - \varepsilon)] = 0.$$

Thus, for example, in case of a third degree approximation,

$$y_s \leq y_k$$

represents a necessary condition where  $y_k$  is the minor absolute value real root of the following quadratic equation:

$$\begin{aligned} \frac{1}{2} \left[ \frac{\partial^2 v_x}{\partial x^2} (x) - \frac{\partial}{\partial x} \frac{D_f(x) + D_a(x)}{2} + \frac{\partial \Omega}{\partial y} (x) \right] y_k^2 (x) - \\ - \left[ \frac{\partial v_y}{\partial x} (x) - \Omega (x) \right] y_k (x) - v_x (x) = 0. \end{aligned} \quad (24)$$

If Equation (24) has no real root,  $y_s$  is not restricted.

This approximation, that is, taking only the first member of the right hand side of Equation (23) when calculating  $q_x(x)$ , represents the classical employment of the chord as a singularity carrier [5, 6].

If a better approximation of function  $q_x(x)$  is required, more members of the right hand side of Equation (23) must be taken into consideration. Since these also depend on  $y_s$ , solution is by iteration. In this connection, the  $(j + 1)$  approximation of  $y_s$  is obtained from its  $j$  approximation in such a manner where, with the  $j$  approximation known, the  $(j + 1)$  approximation of distribution  $q_x(x)$  is obtained as the solution of Equation (23), and this is used to calculate the  $(j + 1)$  approximation of the induced velocities by making use of Equations (12). This is followed by the calculation of  $\alpha$ , then that of  $v_x$  and  $v_y$  and their derivatives then again, on the basis of Equation (20), the  $(j + 1)$  approximation of  $y_s$ . This may be repeated until the  $j$  and  $(j + 1)$  approximations of  $y_s$  sufficiently agree.

### Blade thickness

Blade thickness is determined by distribution  $q_s(s)$ . In the calculation described above, the effect of this is manifested in distribution  $q_x(x)$  as shown by Equations (22) and (23). Blade thickness could be taken into account in

one of two different ways. According to the first method, function  $F(x)$  is assumed on the basis of practical experiences or specified through Equation (22) on the basis of assuming the  $b(s)q_s(s)$  series, and then the thus obtained blade thickness is calculated. The other possibility is to calculate distribution  $F(x)$  for a specified blade thickness distribution. Since thin blades have been assumed, the latter case will be dealt with in detail.

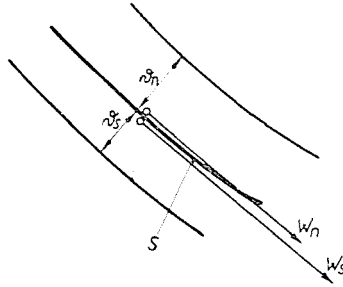


Fig. 4

Assuming a blade thickness  $\vartheta$  at the  $P$  point of singularity carrier  $S$  (Fig. 4) in plane  $\zeta$  and, its equivalent on the  $A-A$  surface within the impeller (Fig. 1), a blade thickness  $\tau$ . In case of thin blades, the approximation

$$\vartheta \cong \tau \frac{zt}{2r\pi} \quad (25)$$

is permissible, and now let us assume that  $\vartheta = \vartheta_n + \vartheta_s$ . By making use of the following approximation as expressed with the symbols of Fig. 4:

$$w_n \vartheta_n \approx w_s \vartheta_s \approx \frac{1}{b(x)} \int_0^S b(s) \frac{q_s(s)}{2} ds, \quad (26)$$

and employing expression (22), the following approximation may be written:

$$F(x) \cong 2\vartheta \frac{w_n w_s}{w_n + w_s} \quad (27)$$

where approximations

$$w_n = \sqrt{1 + y'_s(x)^2} w_{xf} - y'_s(x) \frac{q_s}{2} \approx \sqrt{1 + y'_s(x)^2} w_{xf} \quad (28/a)$$

and

$$w_s \cong \sqrt{1 + y'_s(x)^2} w_{xa} \quad (28/b)$$

are permissible. Finally, applying the usual expansion, expressions

$$w_{xf} \cong v_x - \frac{\gamma_x}{2} + \left[ \frac{\partial}{\partial x} \left( v_y + \frac{q_x}{2} \right) - \Omega \right] y_s + \left[ \frac{\partial^2}{\partial x^2} \left( \frac{\gamma_x}{2} - v_x \right) + \frac{\partial}{\partial x} D_f - \frac{\partial \Omega}{\partial y} \right] \frac{y_s^2}{2} \quad (29/a)$$

and

$$w_{xa} \cong v_x + \frac{\gamma_x}{2} + \left[ \frac{\partial}{\partial x} \left( v_y - \frac{q_x}{2} \right) - \Omega \right] y_s + \left[ \frac{\partial^2}{\partial x^2} \left( \frac{\gamma_x}{2} + v_x \right) + \frac{\partial}{\partial x} D_a - \frac{\partial \Omega}{\partial y} \right] \frac{y_s^2}{2} \quad (29/b)$$

may be written.

If, in order to satisfy Equation (23), function  $q_x(x)$  ought to be determined by the iteration described in the previous chapter, then there is no reason why the desired  $F(x)$  distribution could not be gradually approximated either, by making use of Equations (29), (28) and finally, (27). The  $q_x(x)$  distribution employed would, thereby, correspond to the specified  $\tau(s)$  thickness distribution.

According to experiences in numerical calculations gathered, iteration would converge in a rapid rate as illustrated by the following example. A fully radial flow impeller had  $n_{qe} \cong 18.1$  and  $\psi_e \cong 1.37$ ; with the blade profile given in polar coordinates, the maximum relative error as compared to the final situation was, after the first step,  $-0.014$  radially and  $0.007$  angularly, and after the second step  $-0.002$  radially and  $0.001$  angularly. At the same time the average relative error, that is, the sum of the relative errors of the counted points divided by the number of these points, was after the zeroth step  $+0.008$  radially and  $0.003$  angularly, then after the first step  $0.0014$  radially and  $0.0007$  angularly and, finally, after the second step  $0.0009$  radially and  $0.0003$  angularly.

### Determination of the blade profile

By means of the method described in the previous chapters the physically feasible singularity carrier curve  $S$  can be accurately determined in plane  $\zeta$ . The mapping out defined by Equations (1) makes the determination of the image of  $S$ -curve within the impeller possible, that is, the  $S_k$  curve as well as its  $r_s$  and  $\varphi_s$  coordinates, on the  $A-A$  surface (Fig. 1). Now, regarding coordinates  $r_s$  and  $\varphi_s$  as known, determination of the blade section profile points will be dealt with.

Blade thickness  $\tau$  is known at each point of curve  $S_k$  as it was a starting point for the calculations. Let pressure be at side thickness  $\tau_n$ , and suction side thickness  $\tau_s$ . Accordingly

$$\tau = \tau_n + \tau_s \quad (30)$$

and according to expression (26)

$$\tau_n w_n \approx \tau_s w_s \quad (31)$$

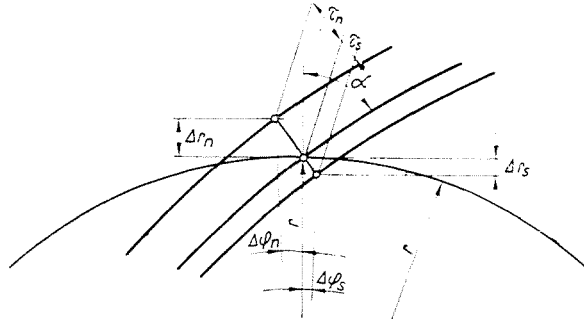


Fig. 5

that is,

$$\tau_n = \frac{\tau}{1 + \frac{w_n}{w_s}} \quad (32)$$

and  $\tau_s = \tau - \tau_n$ .

Since thicknesses  $\tau_n$  and  $\tau_s$  must be measured as normal to curve  $S_k$ , obviously none of the  $r_s$  and  $\varphi_s$  coordinates of any point pertaining to curve  $S_k$  would be identical to any of the coordinates of the profile point sought for but using the symbols of Fig. 5, they could be expressed as

$$r_{kn} = r_s + \Delta r_n \quad \text{and} \quad \varphi_{kn} = \varphi_s + \Delta \varphi_n \quad (33/a)$$

and

$$r_{ks} = r_s + \Delta r_s \quad \text{and} \quad \varphi_{ks} = \varphi_s + \Delta \varphi_s. \quad (33/b)$$

On the basis of Fig. 5, if  $\tan \alpha < 0$  and with Fig. 1 taken into consideration also

$$\Delta r_n = \tau_n \frac{-\tan \alpha}{\sqrt{1 + \tan^2 \alpha}} \sin \delta \quad (34/a)$$

that is,

$$\Delta r_s = \tau_s \frac{\tan \alpha}{\sqrt{1 + \tan^2 \alpha}} \sin \delta \quad (34/b)$$

and

$$\Delta\varphi_n = \frac{\tau_n}{r_s \sqrt{1 + \tan^2 \alpha}} \quad (35/a)$$

that is

$$\Delta\varphi_s = \frac{-\tau_s}{r_s \sqrt{1 + \tan^2 \alpha}} \quad (35/b)$$

In each relation

$$\tan \alpha = \frac{\frac{\eta_2}{\xi_2} + y'_s(x)}{1 - \frac{\eta_2}{\xi_2} y'_s(x)} \quad (36)$$

where all data are known.

Having the singularity carrier  $S$  in plane  $\zeta$  determined, coordinates  $r$  and  $\varphi$  can be determined for any of its points on the basis of Equations (1) then, by making use of Equations (36), (35), (34) and (33) coordinates  $r_{kn}$  and  $\varphi_{kn}$  as well as coordinates  $r_{ks}$  and  $\varphi_{ks}$  may be similarly calculated. This makes the blade sections on the assumed surface of revolution known.

Velocity distribution along the blade section is calculated in the usual manner [4].

### Summary

The paper makes use of the possibilities offered by the singularity carrier auxiliary curve to facilitate the design of bladings for narrow radial flow impellers and guide wheels.

Since narrow impellers are being dealt with, investigations are limited to the determination of the sections of blades on an axisymmetric stream surface. The thickness of the thin blades may be specified, and a rapidly converging relatively simple iteration method is described for the determination of the source distribution.

### References

1. FÚZY, O.: The employment of singularity carrier auxiliary curves for blade profile design. *Per. Polytechnica* **X**, 223 (1966).
2. CZIBERE, T.: Berechnungsverfahren zum Entwurf radialer Schaufelgitter. *Acta Techn. Hung.* **38**, (1962).
3. CZIBERE, T.: Über die Berechnung der Schaufelprofile von Strömungsmaschinen mit halb-axialer Durchströmung. *Acta Techn. Hung.* **44**, (1963).
4. FÚZY, O.: Design of Mixed Flow Impeller. *Per. Polytechnica* **VI**, (1963).
5. KRÜGER, H.: Ein Verfahren zur Druckverteilungsrechnung an geraden und radialen Schaufelgittern. *Ing. Arch.* **27**, (1958).
6. GRUBER, J.: Die Konstruktion von Schaufelsternen mit rückwärts gekrümmter Beschau- felung. *Per. Polytechnica* **I**, (1957).
7. FÚZY, O.: Design of straight cascades of slightly curved bladings by means of singularity carrier auxiliary curve. *Per. Polytechn.* **X**, 335 (1966).
8. FÚZY, O.: Blading design for near-radial flow impellers (in Hungarian). *BME Tud. Évk.* (Sci. Yearbook of the Budapest Techn. Univ.) 1961.

Dr. Olivér FÚZY, Budapest XI., Sztoczek u. 2-4. Hungary.